Characterization of cladded glass fibers using acoustic microscopy

doi: 10.1063/1.102006

Characterization of cladded glass fibers using acoustic microscopy

C. K. Jen, C. Neron, J. F. Bussiere, L. Li,[a] R. Lowe,[b] and J. Kushibiki[c]
Industrial Materials Research Institute, National Research Council of Canada, Boucherville, Quebec J4B 6Y4, Canada

(Received 16 June 1989; accepted for publication 3 October 1989)

Spatial distribution profiles of leaky surface acoustic wave velocity (V_{LSAW}) and attenuation across the diameters of cladded glass fibers are presented. The profiles are obtained by using a novel $V(x,z)$ analysis with a reflection scanning acoustic microscope operated at 775 MHz, and are compared with optical refractive index profiles. Optical fibers with different dopants and dopant concentrations have been investigated. The role of acoustic property profiles in the design of optical and acoustic fibers is outlined.

Pure and doped fused silica glasses are widely used as core and cladding materials for cladded optical fibers. Their acoustic properties are of much importance[1] because (i) depending on the acoustic velocity profile between core and cladding the threshold of stimulated Brillouin backward scattering, which principally limits the maximum transmittable optical power in long single-mode optical fibers,[2] may be different by a factor of 15[3]; and (ii) acoustically induced phase modulation in single-mode optical fibers has been of interest for sensor and telecommunication applications.[4,5] Cladded acoustic fibers[6,7] can also be made of these glasses and the acoustic guidance of the propagating acoustic waves intimately depends on the acoustic profile across the fiber diameter.

Acoustic properties of cladded fibers have been studied previously by Brillouin scattering[4] and acoustic standing-wave resonance methods,[5] but only averaged bulk acoustic wave (BAW) velocities could be obtained. Although scanning acoustic microscope (SAM) images (amplitude) of different types of fibers have been reported[8] which show qualitatively the presence of gradients in acoustic properties, quantitative results were limited by phase reversal phenomena of SAM images[8,9] and by the potentially large error in the determination of acoustic impedance using reflection coefficients (amplitude) at the liquid-solid interface with a highly focused acoustic beam.[10] In addition, quantitative elastic constants of several different glasses in bulk form have been studied by $V(z)$ curves of a line-focus SAM.[11] In this letter a novel $V(z)$ analysis using a reflection acoustic microscope operated at 775 MHz is employed to obtain the leaky surface acoustic wave (LSAW) velocity and attenuation profiles across fiber diameters. These are then compared with the optical refractive index distribution of cladded fibers.

The principles of reflection SAM and $V(z)$ curve measurements where $V(z)$ is the voltage response of the piezoelectric transducer of the SAM lens while the lens is moving toward the sample or vice versa along the lens axis direction z are well documented.[12,13] Our technique records $V(z)$ curves while scanning an arbitrary x axis along the surface of the sample; a $V(x,z)$ plane is then obtained. Figure 1(a) shows a transmission optical image of a cladded glass fiber consisting of two doped core regions. Figure 1(b) is the $V(x,z)$ curve measured along a horizontal line across the middle of Fig. 1(a). In Fig. 1(b), the horizontal and the vertical axes correspond to x and $-z$, respectively, and the brightness is proportional to V. At each x value one $V(z)$ curve can be displayed along the vertical, $-z$ axis direction. Figure 2 shows three $V(z)$ curves at three different x positions indicated in Fig. 1(b). The $V(z)$ curve at each x position is processed by a Fourier analysis technique including a fast Fourier transform (FFT).[13]

The beat (oscillatory) pattern in Fig. 2 gives rise to the bright and dark regions in Fig. 1(b). The distance between the periodic dips is known as Δz. The relation between veloc-

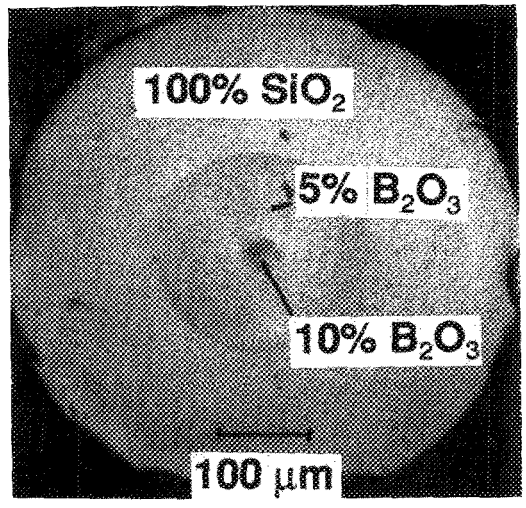

(a)

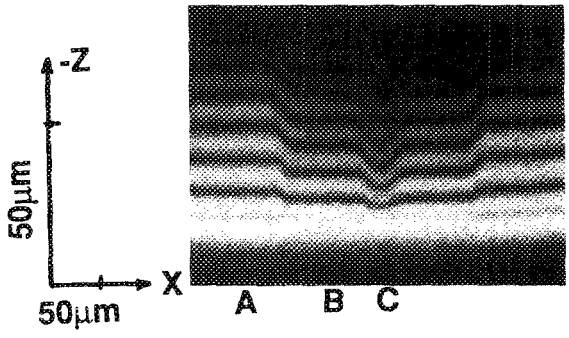

(b)

FIG. 1. (a) Transmission optical micrograph of a cladded glass fiber, (b) $V(x,z)$ plane across the center of fiber in (a).

[a] Department of Electronics and Computer Science, The University, Southampton SO9 5NH, U. K.
[b] Optical Cable Division, Northern Telecom Ltd., Saskatoon, Saskachewan S7K 3L7, Canada.
[c] Department of Electrical Engineering, Tohoku University, Sendai 980, Japan.

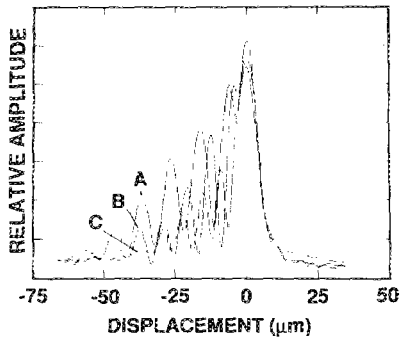

FIG. 2. $V(z)$ curves obtained at three different x positions in Fig. 1(b).

ity v_{LSAW} of leaky surface acoustic wave (LSAW) and Δz is given as

$$v_{LSAW} = v_l / [1 - (1 - v_l / 2f\Delta z)^2]^{1/2}, \quad (1)$$

where v_l is the velocity of the water couplant and f is the ultrasonic frequency (775 MHz). For our samples larger Δz refers to higher v_{LSAW}.

Before the FFT processing, the low-frequency background of the $V(z)$ curve (arising from the SAM lens response) must be removed. Usually, this is performed using a calibration procedure of the lens with the help of a material such as lead or Teflon supporting no leaky surface wave.[13] In our experiments, we used a different approach in which the low-frequency background was removed with a high-pass numerical filter, consisting of a first-order differentiation of the $V(z)$ curves.[14] After the FFT processing of this trace the spatial frequency spectrum versus the wave number k (rad/μm) is obtained. The v_{LSAW} is then deduced from the wave number at the peak of this spectrum,[13,14] and the attenuation α_{LSAW} of LSAW from the width of this spectrum.[13] The v_{LSAW} and α_{LSAW} profiles deduced from $V(x,z)$ curves shown in Fig. 1(b) are given in Figs. 3(a) and 3(b), respectively. The relative accuracy of v_{LSAW} and α_{LSAW} measurements is limited to approximately 2% and 10 dB/mm, respectively, due to the imperfect fiber polishing. At boundaries between two regions of different elastic properties a reduced measurement accuracy was observed. Since the contrast of acoustic images among regions of different elastic properties changes with $-z$ position (phase reversal phenomena[8,9]), only one, at $z = -6\,\mu$m, is given in Fig. 4 as a reference. From Fig. 1(b) this phenomenon can be verified with ease. The image contrast at each different $-z$ for the scanned x line corresponds to the contrast of $V(x, -z)$. In addition, the optical refractive index profile of this fiber, measured at the preform stage (i.e., before fiber drawing) is illustrated in Fig. 5 for comparison purposes. In Fig. 5, Δn for pure fused silica is equal to zero.

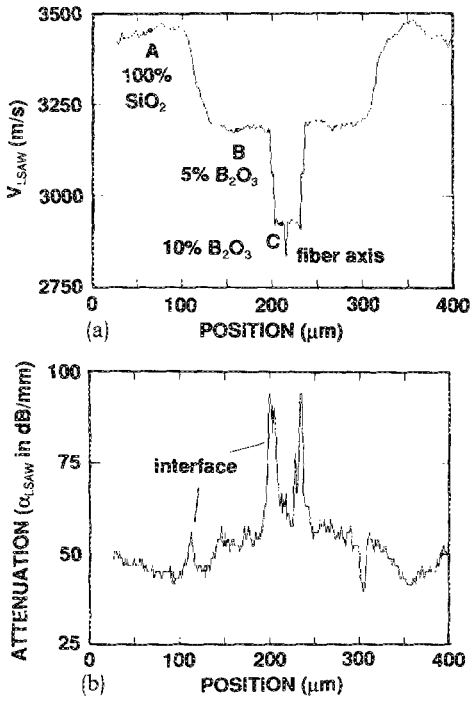

FIG. 3. (a) V_{LSAW} profile and (b) α_{LSAW} profile of Fig. 1(b).

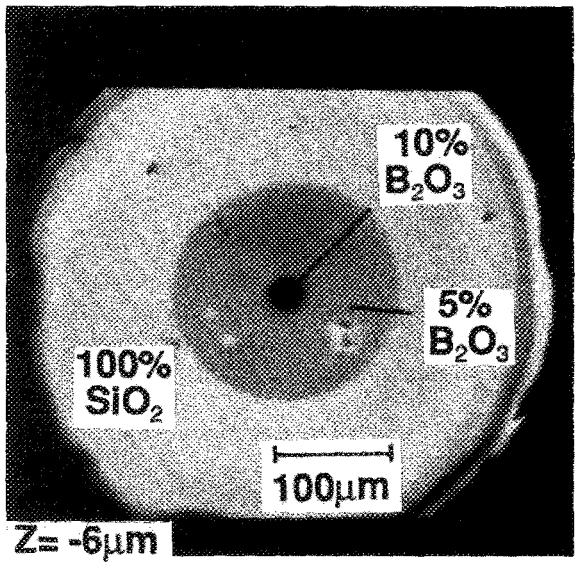

FIG. 4. Acoustic micrograph at $z = -6\,\mu$m.

Several cladded glass fibers obtained from different fiber suppliers were used as samples. The description of these fibers is given in Table I. The criterion for being an "optical fiber" or an "acoustic fiber" in the last two columns of Table I is that the phase velocity of the fiber core is less than that of the fiber cladding. Fiber A was used as a demonstration for the $V(x,z)$ analysis in the previous section. Before SAM studies all fiber end surfaces were polished. The resolution of the 775 MHz SAM at focus is 2 μm, but due to the defocusing mechanism during $V(z)$ measurements, v_{LSAW} and its attenuation profiles, shown in Figs. 3(a) and 3(b), respectively, at a particular x_0 position, is in fact an averaged value around x_0, which extends over a region of $\sim 10\,\mu$m diameter. Therefore, at the boundary between different dopant con-

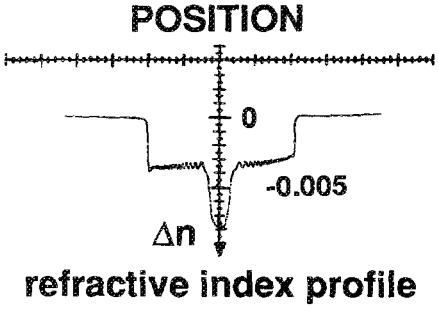

FIG. 5. Optical refractive index profile.

TABLE I. Glass fiber description. (-) means unknown percentage.

	Core dopant (%)	Cladding dopant (%)	Core radius (μm)	Clad. thickness (μm)	Optical fiber	Acoustic fiber
A	B_2O_3(10) inner B_2O_3(5) outer	SiO_2 (100)	25 100	150	No	Yes
B	GeO_2(6) inner GeO_2(6)/P_2O_5(-)/F_2(0.02) outer	SiO_2 (100)	75	75	Yes	Yes
C	GeO_2(6) inner P_2O_5(0.75)/F_2(0.25) outer B_2O_3(10)	SiO_2 (100)	oval (> 10) oval (> 35) Bowtie	> 200	Yes Bowtie fiber[a]	Yes
D	SiO_2 (100%)	F_2(-)	100	20	Yes	No
E	TiO_2(7.5)	SiO_2 (100)	oval (> 80)	75	Yes	Yes

[a] Reference 16.

centrations the variation of v_{LSAW} profiles is not as sharp as observed for the optical refractive index distribution.

Using the same $V(x,z)$ analysis described in the previous section, fibers *B–E* consisting of different dopants and dopant concentrations as listed in Table I were investigated. As shown in Table II the effect of the various dopants studied is to cause a decrease of velocity with respect to pure fused silica. The above observation on the tendency of the variation of v_{LSAW} is consistent with reported bulk longitudinal v_L and shear wave velocity v_S data collected in Ref. 15. For instance, the B_2O_3 dopant reduces v_L and v_S, and also v_{LSAW}. It is believed that v_L and v_S profiles could be used as acoustic design criteria for optical and acoustic fibers,[1] and it is expected that v_{LSAW} profile may be used as an alternative. In Table II the variation of the inverse of the refractive index, $1/n$, is indicated for comparison purposes.

It is very interesting to note that a sharp dip in the measured v_{LSAW} shown in Fig. 3(a) is observed at the fiber axis. A similar abrupt variation also appears in the refractive index profile shown in Fig. 5. This dip region is produced during the fiber preform fabrication process using the modified chemical vapor deposition (MCVD) method. Such a preform, consisting of core and cladding regions, is made from a "collapse" process, in which a tubular structure is collapsed into a rod shape.[17] The similar dip in v_{LSAW} profiles was also observed for fibers *B*, *C*, and *E* fabricated by the MCVD method, but not for fiber *D*, fabricated by a process with no collapse step.

Figure 3(b) indicates that the α_{LSAW} is higher at the interface between two regions of different dopant concentrations. The main reason is the acoustic scattering at this interface because of the elastic discontinuity. As expected α_{LSAW} of pure fused silica regions is less than that of regions having dopants. Further studies on the effects of α_{LSAW} on the performance of optical and acoustic fibers will be performed.

TABLE II. Variation of V_{LSAW} and $1/n$ for different doped fused silica indicated in Table I.

	GeO_2	B_2O_3	F_2	TiO_2	F_2/P_2O_5
V_{LSAW}	↓	↓	↓	↓	↓
$1/n$	↓	↑	↑	↓	↑

A novel $V(x,z)$ analysis with a reflection scanning acoustic microscope operated at 775 MHz has been used to obtain the leaky surface acoustic wave velocity v_{LSAW} and attenuation profiles of cladded glass fibers of different dopants and dopant concentrations. It has been shown that for all the samples studied the effect of added dopants on the variation of bulk acoustic wave properties of pure fused silica has the same tendency as that on v_{LSAW}. Therefore, v_{LSAW} profiles could be used as an alternative acoustic design criterion for optical and acoustic fibers.

Preform and fiber fabrications of fibers *A* and *C* from A. Smithson and R. McGowan of Southampton University at U. K. and fiber *D* from K. Abe of National Optics Institute at Quebec are appreciated.

[1] C. K. Jen, J. E. B. Oliveira, N. Goto, and K. Abe, Electron. Lett. **24**, 1419 (1988).
[2] R. G. Smith, Appl. Opt. **11**, 2489 (1972).
[3] R. H. Stolen, IEEE J. Quantum Electron. **QE-15**, 1157 (1979).
[4] N. Lagakos, J. A. Bucaro, and R. Hughes, Appl. Opt. **19**, 3668 (1980).
[5] F. S. Hickernell, Proc. IEEE Ultrason. Symp. 417 (1988).
[6] G. D. Boyd, L. A. Coldren, and R. N. Thurston, IEEE Trans. Sonics Ultrason. **SU-24**, 246 (1977).
[7] C. K. Jen, Proc. IEEE Ultrason. Symp. 443 (1987).
[8] C. K. Jen, J. F. Bussiere, G. W. Farnell, and R. D. Kinsella, Electron. Lett. **19**, 922 (1983).
[9] R. D. Weglein and R. G. Wilson, Electron Lett. **14**, 352 (1978).
[10] K. K. Liang, Proc. IEEE Ultrason. Symp. 1141 (1987).
[11] J. Kushibiki, T. Ueda, and N. Chubachi, Proc. IEEE Ultrason. Symp. 817 (1987).
[12] A. Atalar, J. Appl. Phys. **49**, 5130 (1978).
[13] J. Kushibiki and N. Chubachi, IEEE Trans. Sonics Ultrason. **SU-32**, 189 (1985).
[14] J. Y. Duquesne, K. Yamanaka, C. Neron, C. K. Jen, L. Piche, and G. Lessard, Proc. Materials Res. Soc. Conf. Symp. U.: Nondestructive Characterization of Materials, Boston, Nov. 1988 (in press).
[15] C. K. Jen, A. Safaai-Jazi, and G. W. Farnell, IEEE Trans. Ultrason. Ferroelectrics Freq. Control **UFFC-33**, 634 (1986).
[16] R. D. Birch, D. N. Payne, and M. P. Varnham, Electron. Lett. **18**, 1036 (1982).
[17] D. Marcuse and H. M. Presby, Proc. IEEE **68**, 666 (1980).